16th International Conference on Information Fusion
Istanbul, Turkey, July 9-12, 2013

Exploiting Amplitude Spatial Coherence for Multi-target Particle Filter in Track-Before-Detect

Alexandre Lepoutre, Olivier Rabaste,
ONERA, Chemin de la Hunière et des Joncherettes,
BP 80100, 91123 PALAISEAU Cedex, France.
E-mail : Alexandre.Lepoutre@onera.fr

François Le Gland,
INRIA Rennes,
Campus de Beaulieu 35042 RENNES Cedex, France.

***Abstract*—In this paper, we address the problem of tracking one or several targets in a Track-Before-Detect (TBD) context using particle filters. These filters require the computation of the likelihood of the complex measurement given the target states. This likelihood depends on the complex amplitudes of the targets. When the complex amplitude fluctuates over time, time coherence of the target cannot be taken into account. However, for the single target case, spatial coherence of this amplitude can be taken into account to improve the filter performance, by marginalizing the likelihood of the complex measurement over the amplitude parameter. The marginalization depends on the fluctuation law considered. We consider in this article *Swerling* 0 and *Swerling* 1 fluctuation models. We show that for the *Swerling* 1 model the likelihood of the complex measurement can be obtained analytically in the multi-target case. For the *Swerling* 0 model no closed form can be obtained in the general multi-target setting. Therefore we resort to some approximations to solve the problem. Finally, we demonstrate with Monte-Carlo simulations the gain of this method both in detection and in estimation compared to the classic method that works with the square modulus of the complex signal.**

I. Introduction

The radar tracking problem consists in detecting and tracking one or several targets from the measurements provided by the radar. Usually, the problem is divided into two steps. First a pre-detection step that consists in thresholding the raw radar data and provides detection "hits" that correspond to potential targets or false alarms. Then, according to these detection "hits", the tracking stage is performed and allows to update, create or delete target tracks. This procedure performs well at high target Signal to Noise Ratios (SNR). However at low SNR, either the detection threshold is chosen too large and the detection probability is then small, or the threshold is set too low, leading to a large false alarm probability that makes the association problem very hard to solve.

To avoid these limits, a new approach, known as Track-Before-Detect (TBD), has been proposed [1]. In this framework, detection and tracking are performed jointly from the raw radar data. As all the information is kept, this strategy is expected to provide better performance for low target SNRs. Unfortunately, due to the non linearity of the measurement equation and possibly to the non Gaussianity of the noise, classic tracking methods based on Kalman filter such as PDAF, JPDAF [2] cannot be used in this context. Thus, to overcome these difficulties, solutions based on particle filters have been proposed in the literature, first in the single target case [3], then in the multiple target case [4]. In these particle filters, the computation of the particle weights requires the computation of the likelihood of the measurement given the particle states, [5] that depends, in radar application, on the complex amplitudes of the targets that are unknown and may fluctuate over time. Generally the phase of the complex amplitude is supposed to be, at each iteration, uniformly distributed over $[0, 2\pi)$ and the modulus is often modeled with *Swerling* models [6]. We consider, in this paper, that target amplitude modulus are either modeled by the *Swerling* 0 model – in this case modulus is assumed constant over time –, or by the *Swerling* 1 model – the modulus is then distributed according to a Rayleigh distribution.

Since these amplitude parameters are unknown, the likelihood of the measurement cannot be computed directly. A first possible solution often encountered in the literature consists in working on the square modulus of the complex measurement [7], thus allowing to remove the dependency on the phase. In that case, if the modulus also fluctuates, the likelihood can be numerically integrated with respect to the modulus fluctuation distribution. Note that, in the *Swerling* 1 case, Boers *et al.* have derived a closed form expression for the likelihood [8]. However, this method does not take into account the fact that the complex amplitude is constant from cell to cell on the overall signal and thus induces a loss of sensitivity of the filters. To avoid such a loss, Davey *et al.* proposed, in the single target case and in the *Swerling* 0 model, to directly marginalize the likelihood of the complex measurement over the phase [9]. In that specific case they obtain a closed form for the likelihood and show a significant gain both in estimation and in detection.

In this paper, we first propose to extend this method to the multi-target case in *Swerling* 0. Unfortunately, in that difficult case, a closed form cannot be obtained analytically for close targets. We therefore propose approximations to solve this problem. Second, we propose to exploit the spatial coherence of the amplitude modulus in the *Swerling* 1 case, that is usually discarded as well in the literature [8]. In that case, we show that a closed form expression can be achieved in the general multi-target case.

This paper is organized as follows. In section II we present the radar signal model. Then in section III we present the classic method to compute the likelihood from the square modulus of the complex signal. In section IV we show that the likelihood can be computed directly from complex measurement in *Swerling* 0 and *Swerling* 1 models. Finally in sections V and VI we present simulation results that show

978-605-86311-1-3 ©2013 ISIF

the gain both in detection and in estimation for this method compared to the classic one.

II. Problem Formulation

In this section we present the framework for tracking targets from complex measurements in a Track-Before-Detect context.

A. Multi-target state

In a Bayesian framework, the aim is to calculate at a given time step k the *a posteriori* density of the hidden state $\mathbf{X}_k$ conditionally to the observation $\mathbf{z}_{1:k}$ (where the notation $1:k$ represents the collection of elements from 1 to k, for instance $\mathbf{z}_{1:k} = \{\mathbf{z}_1, \ldots, \mathbf{z}_k\}$). In a multi-target setting, the hidden state $\mathbf{X}_k$ consists of the concatenation of all the individual target state vectors [4]. So, if we assume at step k that N_t targets are present, the multi-target state is then given by $\mathbf{X}_k = \left[\mathbf{x}_{k,1}^T, \ldots, \mathbf{x}_{k,N_t}^T\right]^T$ (which can also be denoted by $\mathbf{x}_{k,1:N_t}$) where each $\mathbf{x}_{k,i} = [x_{k,i}, \dot{x}_{k,i}, y_{k,i}, \dot{y}_{k,i}]^T$, $i \in \{1, \ldots, N_t\}$, is the individual state of target i at time k that consists of the position and the velocity in Cartesian coordinates.

B. Measurement model

We suppose here that observations consist of range and bearing raw radar data obtained after range matched filtering and adaptive beam forming. Thus, at step k, the measurement $\mathbf{z}_k$ consists of $N = N_r \times N_\theta$ range-bearing cells, with a given resolution Δ_r in range and Δ_θ in bearing. For convenience, we transform $\mathbf{z}_k$ into a vector $\mathbf{z}_k = [z_k^{11}, z_k^{12}, ..., z_k^{lm}, ..., z_k^{N_r N_\theta}]^T$, with z_k^{lm} the signal measured in the range-bearing cell (l, m) (rather than a bi-dimensional array). Then, given the target state $\mathbf{X}_k$, the measurement $\mathbf{z}_k$ is given by the following nonlinear equation:

$$\mathbf{z}_k = \sum_{i=1}^{N_t} \rho_{k,i} e^{j\varphi_{k,i}} \mathbf{h}(\mathbf{x}_{k,i}) + \mathbf{n}_k, \tag{1}$$

where:

- $\mathbf{h}(\mathbf{x}_{k,i})$ represents the 2D range-bearing ambiguity function of the i^{th} target centered on the target location $(x_{k,i}, y_{k,i})$ and unfolded in the same way as $\mathbf{z}_k$. For the sake of clarity, $\mathbf{h}(\mathbf{x}_{k,i})$ will be denoted $\mathbf{h}_{k,i}$ in the rest of the paper.
- $\mathbf{n}_k$ is a circular symmetric complex Gaussian vector with invertible covariance matrix $\mathbf{\Gamma}$.
- $\varphi_{k,i}$ and $\rho_{k,i}$ are respectively the phase and the modulus of the i^{th} target complex amplitude. All variables $\varphi_{k,1:N_t}$ and $\rho_{k,1:N_t}$ are supposed mutually independent, and independent from $\mathbf{n}_k$.

Each phase $\varphi_{k,i}$ is supposed to be unknown and uniformly distributed over the interval $[0, 2\pi)$. Under these conditions, it is not possible to estimate it precisely over time. Concerning the modulus $\rho_{k,i}$, we consider in this article two cases. Either the modulus follows the fluctuation model *Swerling* 0, that is to say it is constant over time, or the fluctuation model *Swerling* 1, in which case the modulus is distributed according to a Rayleigh distribution.

C. Measurement likelihood

Most of the time TBD tracking algorithms require the computation of the likelihood $p(\mathbf{z}_k \mid \mathbf{X}_k)$ of the observation conditionally to the multi-target state. However, the measurement equation (1) does not permit to compute $p(\mathbf{z}_k \mid \mathbf{X}_k)$ as it depends on the unknown parameters $\rho_{k,1:N_t}$ and $\varphi_{k,1:N_t}$. In fact, equation (1) allows us to compute the density $p(\mathbf{z}_k \mid \mathbf{X}_k, \rho_{k,1:N_t}, \varphi_{k,1:N_t})$ which is a circular complex Gaussian density with mean $\mu_k = \sum_{i=1}^{N_t} \rho_{k,i} e^{j\varphi_{k,i}} \mathbf{h}_{k,i}$ and covariance matrix $\mathbf{\Gamma}$, *i.e.*

$$p(\mathbf{z}_k \mid \mathbf{X}_k, \rho_{k,1:N_t}, \varphi_{k,1:N_t}) = \frac{1}{\pi^N \det(\mathbf{\Gamma})} \exp\left\{-(\mathbf{z}_k - \mu_k)^H \mathbf{\Gamma}^{-1} (\mathbf{z}_k - \mu_k)\right\}. \tag{2}$$

Then by developing (2) we obtain the following expression:

$$\begin{aligned} p(\mathbf{z}_k \mid \mathbf{X}_k, \rho_{k,1:N_t}, \varphi_{k,1:N_t}) &= \frac{1}{\pi^N \det(\mathbf{\Gamma})} \exp\left\{-\mathbf{z}_k \mathbf{\Gamma}^{-1} \mathbf{z}_k\right\} \times \\ \exp\Bigg\{ -\sum_{i=1}^{N_t} \rho_{k,i}^2 \mathbf{h}_{k,i}^H \mathbf{\Gamma}^{-1} \mathbf{h}_{k,i} &- \sum_{i=1}^{N_t} 2\rho_{k,i} |\mathbf{h}_{k,i}^H \mathbf{\Gamma}^{-1} \mathbf{z}_k| \cos(\varphi_{k,i} - \xi_{k,i}) \\ - \sum_{i=1}^{N_t} \sum_{l=i+1}^{N_t} 2 \left|\mathbf{h}_{k,i}^H \mathbf{\Gamma}^{-1} \mathbf{h}_{k,l}\right| &\cos(\varphi_{k,i} - \varphi_{k,l} + \phi_{k,il}) \Bigg\}, \end{aligned} \tag{3}$$

where $\xi_{k,i} = \arg\left(\mathbf{h}_{k,i}^H \mathbf{\Gamma}^{-1} \mathbf{z}_k\right)$ and $\phi_{k,il} = \arg\left(\mathbf{h}_{k,i}^H \mathbf{\Gamma}^{-1} \mathbf{h}_{k,l}\right)$. In all cases, the ignorance of the variables $\rho_{k,1:N_t}$ and $\varphi_{k,1:N_t}$ is problematic to compute the likelihood $p(\mathbf{z}_k \mid \mathbf{X}_k)$. So, many authors have proposed different strategies to eliminate these variables from the likelihood.

III. Likelihood computation from square modulus of the complex measurement

The first strategy, very common in the literature, consists in working on real samples instead of complex samples [8], [10]. With a slight abuse of notation, let $|\mathbf{z}_k|^2$ be the vector of square modulus of the complex signal, $|\mathbf{z}_k|^2 = [|z_k^{11}|^2, \ldots, |z_k^{N_r N_\theta}|^2]^T$ and assume that samples are mutually independent. Note that this last assumption imposes $\mathbf{\Gamma} = 2\sigma^2 \mathbf{I}_N$. The density $p(|z_k^{lm}|^2 \mid \mathbf{X}_k, \rho_{k,1:N_t}, \varphi_{k,1:N_t})$ in each cell (l, m) does not depend, in this case, on variables $\varphi_{k,1:N_t}$ and is a non central chi-square distribution with two degrees of freedom, given by:

$$p(|z_k^{lm}|^2 \mid \mathbf{X}_k, \rho_{k,1:N_t}) = \frac{1}{2\sigma^2} \exp\left\{-\frac{|z_k^{lm}|^2}{2\sigma^2} - \frac{\gamma^{lm}}{2}\right\} \mathrm{I}_0\left(\sqrt{\frac{\gamma^{lm}|z_k^{lm}|}{\sigma^2}}\right), \tag{4}$$

where I_0 is the modified Bessel function of the first kind and $\gamma^{lm} = \frac{\sum_{i=1}^{N_t} \rho_{k,i}^2 |h_{k,i}^{lm}|^2}{\sigma^2}$ is the non centrality parameter. Then by integrating with respect to the density $p(\rho_{k,1:N_t})$ [10] which depends on the fluctuation model considered, we obtain

$$p(|z_k^{lm}|^2 \mid \mathbf{X}_k) = \int p(\rho_{k,1:N_t}) p(|z_k^{lm}|^2 \mid \rho_{k,1:N_t}, \mathbf{X}_k) d\rho_{k,1:N_t}. \tag{5}$$

In practice this integral is often intractable and has to be estimated by numerical integration. Finally, the density of $|\mathbf{z}_k|^2$ conditionally on $\mathbf{X}_k$ is given by

$$p(|\mathbf{z}_k|^2 \mid \mathbf{X}_k) = \prod_{l=1}^{N_r} \prod_{m=1}^{N_\theta} p(|z_k^{lm}|^2 \mid \mathbf{X}_k). \tag{6}$$

Note that most of the TBD algorithms require only the computation of the likelihood up to a constant. Therefore, to avoid unnecessary computation it is better to use the likelihood ratio:

$$\mathcal{L}\left(|\mathbf{z}_k|^2 \mid \mathbf{X}_k\right) = \frac{p\left(|\mathbf{z}_k|^2 \mid \mathbf{X}_k\right)}{p_0\left(|\mathbf{z}_k|^2\right)},$$

where $p_0\left(|\mathbf{z}_k|^2\right)$ is the density of $|\mathbf{z}_k|^2$ under the assumption that no target is present, given by

$$p_0\left(|\mathbf{z}_k|^2\right) = \frac{1}{(2\sigma^2)^N} \exp\left\{-\sum_{l=1}^{N_r}\sum_{m=1}^{N_\theta} \frac{|z_k^{lm}|^2}{2\sigma^2}\right\}.$$

Indeed, for pixels far away from the target location, the non centrality parameter γ^{lm} is almost equal to zero and therefore the likelihood ratio can be considered as equal to one. Finally, the overall likelihood ratio can just be computed in the cells where target ambiguity functions remain significant, *i.e.*

$$\mathcal{L}\left(|\mathbf{z}_k|^2 \mid \mathbf{X}_k\right) = \prod_{(l,m)\in\mathcal{V}_k} \mathcal{L}\left(|z_k^{lm}|^2 \mid \mathbf{X}_k\right), \tag{7}$$

where $\mathcal{V}_k$ is the set of pixels where the target ambiguity functions are not negligible.

In the *Swerling* 0 case, the modulus $\rho_{k,i}$ of each target does not fluctuate and is equal to the unknown parameter ρ_i. Consequently, computing the likelihood ratio from the square modulus measurement just consists here in substituting values $\rho_{k,1:N_t}$ by constants $\rho_{1:N_t}$. Although these constants are unknown, they can be estimated over time and the estimates injected into the likelihood ratio. For instance, in particle filter, amplitude parameters $\rho_{1:N_t}$ can be inserted in the state vector, with artificial dynamics, and sampled as the other state parameters [11].

In the *Swerling* 1 model, at each step k, the modulus $\rho_{k,i}$ is distributed according to a Rayleigh distribution

$$p_{SW1}\left(\rho_{k,i}\right) = \frac{\rho_{k,i}}{\sigma_{\rho,i}^2} \exp\left(-\frac{\rho_{k,i}^2}{2\sigma_{\rho,i}^2}\right),$$

where $\sigma_{\rho,i}$ is the parameter of the Rayleigh distribution such that $\mathbb{E}[\rho_{k,i}^2] = 2\sigma_{\rho,i}^2$. Then the integral (5) can be computed analytically. However, it is easier to notice, as did Boers *et al.* in [8], that, when the noise is uncorrelated (*i.e.* $\mathbf{\Gamma} = 2\sigma^2\mathbf{I}_N$), samples $|z_k^{lm}|^2$ are distributed according to an exponential distribution with parameter $2\nu^{lm} = 2\sigma^2 + \sum_{i=1}^{N_t} 2\sigma_{\rho,i}^2 |h_{k,i}^{lm}|^2$. Thus, assuming independent square modulus samples, the likelihood ratio can be written as follows:

$$\mathcal{L}_{SW1}(|\mathbf{z}_k|^2 \mid \mathbf{X}_k) = \prod_{(l,m)\in\mathcal{V}_k} \frac{\sigma^2}{\nu^{lm}} \exp\left(\frac{|z_k^{lm}|^2}{2\sigma^2\nu^{lm}}\left(\sigma^2 - \nu^{lm}\right)\right). \tag{8}$$

IV. Likelihood Computation from Complex Measurement

The computation of the likelihood from square modulus is not optimal in the sense that it does not take into account the spatial coherence of the complex amplitude and that it implicitly makes the hypothesis that phase and modulus are independent from cell to cell, which is not the case. Moreover, this method requires assuming $\mathbf{\Gamma} = 2\sigma^2\mathbf{I}_N$, an hypothesis that is not always verified. For instance, in radar processing, when windowing is used to reduce sidelobes but the signal is still sampled at the signal bandwidth, the mainlobe width is increased and the noise cannot be assumed white anymore. To avoid these drawbacks, Davey *et al.* have proposed in [9] a method for the computation of the likelihood that takes into account the spatial coherence of the phase φ_k and can address spatially correlated noise. However this strategy has been developed only in the single target case and for the *Swerling* 0 model. In this section, we propose to extend this method to the multi-target case and for the *Swerling* 0 model and the *Swerling* 1 model.

A. Single target likelihood ratio computation

In this section, we first consider the single target case. Thus, the subscript i that refers to the target number will be dropped out for simplicity. For a single target, equation (3) becomes

$$p\left(\mathbf{z}_k \mid \mathbf{x}_k, \rho_k, \varphi_k\right) = \frac{1}{\pi^N \det\left(\mathbf{\Gamma}\right)} \exp\left\{-\mathbf{z}_k \mathbf{\Gamma}^{-1}\mathbf{z}_k\right\}\times \\ \exp\left(-\rho_k^2 \mathbf{h}_k^H \mathbf{\Gamma}^{-1}\mathbf{h}_k + 2\rho_k |\mathbf{h}_k^H \mathbf{\Gamma}^{-1}\mathbf{z}_k| \cos(\varphi_k - \xi_k)\right), \tag{9}$$

where $\xi_k = \arg(\mathbf{h}_k^H \mathbf{\Gamma}^{-1}\mathbf{z}_k)$. The likelihood ratio $\mathcal{L}\left(\mathbf{z}_k \mid \mathbf{x}_k, \rho_k, \varphi_k\right)$ is then obtained by dividing (9) by

$$p_0\left(\mathbf{z}_k\right) = \frac{1}{\pi^N \det\left(\mathbf{\Gamma}\right)} \exp\left\{-\mathbf{z}_k \mathbf{\Gamma}^{-1}\mathbf{z}_k\right\}.$$

Davey *et al.* then proposed to integrate this likelihood ratio with respect to the phase distribution (*i.e.* the uniform distribution over $[0, 2\pi)$), leading to the marginalized likelihood ratio:

$$\begin{aligned}\mathcal{L}\left(\mathbf{z}_k \mid \mathbf{x}_k, \rho_k\right) &= \int_0^{2\pi} \mathcal{L}(\mathbf{z}_k|\mathbf{x}_k, \varphi_k, \rho_k) p(\varphi_k) d\varphi_k, \\ &= \exp\left\{-\rho_k^2 \mathbf{h}_k^H \mathbf{\Gamma}^{-1}\mathbf{h}_k\right\} \mathrm{I}_0\left(2\rho_k \left|\mathbf{h}_k^H \mathbf{\Gamma}^{-1}\mathbf{z}_k\right|\right).\end{aligned} \tag{10}$$

Note that the quantity $\left|\mathbf{h}_k^H \mathbf{\Gamma}^{-1}\mathbf{z}_k\right|$ can be approximated by setting a zero value where the vector $\mathbf{h}_k$ has not a significant contribution, thus allowing the computation of $\left|\mathbf{h}_k^H \mathbf{\Gamma}^{-1}\mathbf{z}_k\right|$ only over a small set of pixels in the vicinity of the target.

In *Swerling* 0, the modulus is constant and equal to a certain value ρ. So no further integration is required. The parameter ρ can be estimated similarly than in the square modulus case, for instance by the method presented in [11]. Note that, as highlighted in [9], whereas the square modulus strategy requires the computation of several Bessel functions, here only one Bessel function is required.

We propose now to extend the method of Davey *et al.* to the *Swerling* 1 model. This requires to marginalize the likelihood ratio (10) with respect to the Rayleigh distribution:

$$\begin{aligned}\mathcal{L}_{SW1}(\mathbf{z}_k \mid \mathbf{x}_k) &= \int_0^{\infty} \mathcal{L}(\mathbf{z}_k|\mathbf{x}_k,\rho_k) p_{SW1}(\rho_k) d\rho_k, \\ &= \frac{1}{\sigma_\rho^2}\int_0^{\infty} \rho_k \exp\left(-\rho_k^2\alpha\right) \mathrm{I}_0(\beta\rho_k) d\rho_k,\end{aligned} \tag{11}$$

where $\alpha = \frac{1}{2\sigma_\rho^2} + \mathbf{h}_k^H\boldsymbol{\Gamma}^{-1}\mathbf{h}_k$ and $\beta = 2\left|\mathbf{h}_k^H\boldsymbol{\Gamma}^{-1}\mathbf{z}_k\right|$. This integral can be computed analytically and is equal to

$$\int_0^{\infty} \rho_k \exp\left(-\rho_k^2\alpha\right) \mathrm{I}_0(\beta\rho_k) d\rho_k = \frac{1}{2\alpha}\exp\left(\frac{\beta^2}{4\alpha}\right).$$

Finally the likelihood ratio is given by:

$$\mathcal{L}_{SW1}(\mathbf{z}_k \mid \mathbf{x}_k) = \frac{1}{1+2\sigma_\rho^2\mathbf{h}_k^H\boldsymbol{\Gamma}^{-1}\mathbf{h}_k}\exp\left(\frac{2\sigma_\rho^2|\mathbf{h}_k^H\boldsymbol{\Gamma}^{-1}\mathbf{z}_k|^2}{1+2\sigma_\rho^2\mathbf{h}_k^H\boldsymbol{\Gamma}^{-1}\mathbf{h}_k}\right). \tag{12}$$

B. Multi-target likelihood ratio computation for distant targets (Swerling 0 and Swerling 1)

As we said previously, the vector $\mathbf{h}_{k,i}$ can be approximated by setting zeros in all cells where the ambiguity function is almost zero. Then, if all targets are far away from each other and if the noise spatial correlation decreases rapidly, we have,

$$\left|\mathbf{h}_{k,i}^H\boldsymbol{\Gamma}^{-1}\mathbf{h}_{k,l}\right| \approx 0,\ \forall\ i,l \in \{1,\ldots,N_t\}.$$

Thus the likelihood ratio becomes the product of the individual target likelihood ratios and, as all variables $\rho_{k,1:N_t}$ and $\varphi_{k,1:N_t}$ are assumed mutually independent, the marginalized likelihood ratio is just the product of the individual marginalized likelihood ratios:

$$\begin{aligned}\mathcal{L}(\mathbf{z}_k \mid \mathbf{x}_{k,1:N_t}) &= \prod_{i=1}^{N_t}\int_0^{2\pi}\int_0^{\infty}\mathcal{L}(\mathbf{z}_k|\mathbf{x}_{k,i},\rho_{k,i},\varphi_{k,i})\, d\varphi_{k,i}d\rho_{k,i}, \\ &= \prod_{i=1}^{N_t}\mathcal{L}(\mathbf{z}_k \mid \mathbf{x}_{k,i}).\end{aligned} \tag{13}$$

This is an interesting property because most of the time targets are well separated and in this case, the multi-target likelihood ratio is just the product of the single target likelihood ratios of the different targets taken individually, thus reducing the computational cost.

C. Multi-target likelihood ratio computation for close targets in Swerling 0 model

When targets are close to each other, the assumption that $\left|\mathbf{h}_{k,i}^H\boldsymbol{\Gamma}^{-1}\mathbf{h}_{k,l}\right| \approx 0,\ \forall\ i,l \in \{1,\ldots,N_t\}$ is not valid anymore and we cannot consider the overall likelihood ratio as the product of the single target likelihood ratios. Unfortunately, marginalizing over phases $\varphi_{k,1:N_t}$ leads to an intractable expression, even for two targets. Then an approximation must be used to compute the likelihood ratio. A first solution is to do a numerical integration over the domain $[0,2\pi)^{N_t}$. However, this solution is computationally intensive and the size of the integration domain increases exponentially with the number of targets. To avoid this drawback, we propose a quite simple approximation based on importance sampling. The marginalized likelihood ratio can be seen as an expectation:

$$\mathcal{L}_{SW0}(\mathbf{z}_k \mid \mathbf{x}_{k,1:Nt},\rho_{1:N_t}) = \mathbb{E}_{p(\varphi_{k,1:N_t})}\left[\mathcal{L}(\mathbf{z}_k \mid \mathbf{x}_{k,1:Nt},\varphi_{k,1:N_t},\rho_{1:N_t})\right],$$

and the approximation in this case is given by,

$$\mathcal{L}_{SW0}(\mathbf{z}_k \mid \mathbf{x}_{k,1:Nt},\rho_{1:N_t}) \approx \sum_{u=1}^{N_{IS}}\frac{p\left(\varphi_{k,1}^u\right)\ldots p\left(\varphi_{k,N_t}^u\right)}{q_1\left(\varphi_{k,1}^u\right)\ldots q_{N_t}\left(\varphi_{k,N_t}^u\right)}\mathcal{L}\left(\mathbf{z}_k \mid \mathbf{x}_{k,1:Nt},\varphi_{k,1:N_t}^u,\rho_{1:N_t}\right), \tag{14}$$

where N_{IS} is the number of samples and $q_i(.)$ is the instrumental density used to draw samples $\varphi_{k,i}^u$. We propose as instrumental density for each variable $\varphi_{k,i}$ the uniform distribution over the interval $[-\delta_\varphi+\widehat{\varphi}_{k,i},\widehat{\varphi}_{k,i}+\delta_\varphi]$, where $\widehat{\varphi}_{k,i}$ is an estimator of $\varphi_{k,i}$. Concerning this estimator, in the general N_t target case ($N_t \geq 2$), the maximum likelihood estimator cannot be computed analytically from (3). It can be obtained by a gradient descent method but this solution is computationally expensive. We therefore propose to use a different estimator. Let $\mathbf{H}_k = [\rho_1\mathbf{h}_{k,1},\ldots,\rho_{N_t}\mathbf{h}_{k,N_t}]$ and let $\Psi_k = [e^{j\varphi_{k,1}},\ldots,e^{j\varphi_{k,N_t}}]^T$. Equation (2) can be rewritten as follows:

$$p(\mathbf{z}_k \mid \mathbf{X}_k,\rho_{1:N_t},\varphi_{k,1:N_t}) = \frac{1}{\pi^N\det(\boldsymbol{\Gamma})}\exp\left\{-(\mathbf{z}_k-\mathbf{H}_k\Psi_k)^H\boldsymbol{\Gamma}^{-1}(\mathbf{z}_k-\mathbf{H}_k\Psi_k)\right\}.$$

Then maximizing with respect to the vector Ψ_k leads to the classic least square estimator

$$\widehat{\Psi}_k = \left(\mathbf{H}_k^H\boldsymbol{\Gamma}^{-1}\mathbf{H}_k\right)^{-1}\mathbf{H}_k^H\boldsymbol{\Gamma}^{-1}\mathbf{z}_k. \tag{15}$$

Note that each component $\widehat{\Psi}_{k,i}$ of vector $\widehat{\Psi}_k$ does not respect the constraint $|\widehat{\Psi}_{k,i}| = 1$. Therefore, this estimator is clearly not the maximum likelihood estimator for the phases $\varphi_{k,1:N_t}$, but it is relatively close to it. Thus, we propose to estimate the phase $\varphi_{k,i}$ by

$$\widehat{\varphi}_{k,i} = \arg\left(\widehat{\Psi}_{k,i}\right). \tag{16}$$

Obviously, the proposed method should lead to slightly worse performance in terms of estimation than the numerical integration but it is much faster. Moreover the number of operations of this method evolves linearly with the number of targets.

D. Multi-target likelihood ratio computation for the Swerling 1 model

In the *Swerling* 1 model, each variable $\rho_{k,i}e^{j\varphi_{k,i}}$ in the measurement equation (1) is a zero-mean circular symmetric complex Gaussian variable with variance $2\sigma_{\rho,i}^2$ (*i.e.* $\rho_{k,i}$ follows a Rayleigh distribution of parameter $\sigma_{\rho,i}^2$ and $\varphi_{k,i}$ is uniformly distributed over $[0,2\pi)$). Therefore the vector $\rho_{k,i}e^{j\varphi_{k,i}}\mathbf{h}_{k,i}$ is also complex Gaussian with zero-mean and covariance matrix $2\sigma_{\rho,i}^2\mathbf{h}_{k,i}\mathbf{h}_{k,i}^H$. Since $\mathbf{z}_k$ is the sum of independent Gaussian vectors with zero-mean, it is also a complex Gaussian vector with zero-mean and covariance matrix $\boldsymbol{\Sigma}_{N_t}$ given by

$$\boldsymbol{\Sigma}_{N_t} = \boldsymbol{\Gamma} + \sum_{i=1}^{N_t} 2\sigma_{\rho,i}^2\mathbf{h}_{k,i}\mathbf{h}_{k,i}^H. \tag{17}$$

Clearly, this matrix is definite positive, so that the multi-target likelihood ratio is finally given in closed form by:

$$\mathcal{L}_{SW1}(\mathbf{z}_k \mid \mathbf{X}_k) = \frac{\det(\mathbf{\Gamma})}{\det(\mathbf{\Sigma}_{N_t})} \exp\left(-\mathbf{z}_k^H \left(\mathbf{\Sigma}_{N_t}^{-1} - \mathbf{\Gamma}^{-1}\right)\mathbf{z}_k\right). \tag{18}$$

Note that here we have not made any hypothesis about the closeness of the targets and therefore this closed form expression is valid both for distant and close targets. However when targets are well separated, it is faster to compute the likelihood ratio of each target individually with (12) because it does not require the computation of the determinant $\det(\mathbf{\Sigma}_{N_t})$ and the inversion of the matrix $\mathbf{\Sigma}_{N_t}$ that can be costly.

V. Single target simulations and results

We compare performance in detection and in estimation with a particle filter that either computes weights from square modulus measurements, or directly from complex measurements. For the *Swerling* 0 model, Davey *et al.* have already shown the gain in detection and in estimation by using integrated likelihood ratio instead of square modulus measurements [9], so we focus here only on the *Swerling* 1 model.

A. Radar signal

We consider a range and bearing surveillance radar that covers the area defined, in polar coordinates, by the pavement $[r_{min}, r_{max}] \times [\theta_{min}, \theta_{max}]$. The radar transmits, at each iteration, a linear frequency modulated signal (

$$h_r^l(\mathbf{x}_k) = \bullet_{\,|\tau^l| \leq T_e} \left| \left(1 - \frac{|\tau^l|}{T_e}\right) \frac{\sin\left(\pi B \tau^l \left(1 - \frac{|\tau^l|}{T_e}\right)\right)}{\pi B \tau^l \left(1 - \frac{|\tau^l|}{T_e}\right)} \right|,$$

with $\tau^l = (r_k - r_l)\,\frac{2}{c}$, c the celerity of the electromagnetic wave, $r_k = \sqrt{x_k^2 + y_k^2}$ the range between the radar and the target and r_l the range of the cell considered. At the reception side the radar consists of a linear phased array with N_a antennas spaced by $\frac{\lambda}{2}$ where λ is the wavelength of the carrier frequency. Finally the ambiguity function along the bearing axis is given by [12]:

$$h_\theta^m(\mathbf{x}_k) = \frac{\sin\left(\frac{N_\bullet \Phi^m}{2}\right)}{N_a \sin\left(\frac{\Phi^m}{2}\right)},$$

with $\Phi^m = \frac{2\pi d_\bullet}{\lambda}\left[\cos(\theta_k) - \cos(\theta_m)\right]$, $\theta_k = \arctan(\frac{y_k}{x_k})$ the target bearing and θ_m the cell bearing. Finally, the range-bearing ambiguity function in cell (l, m) can be expressed as $h^{lm}(\mathbf{x}_k) = h_r^l(\mathbf{x}_k) \times h_\theta^m(\mathbf{x}_k)$.

B. Single target scenario

We consider here a point target with a rectilinear trajectory and a constant velocity uniformly drawn in $[v_{min}, v_{max}]$. The target SNR is defined as $\text{SNR} = 10\log_{10}\left(\frac{2\sigma_\bullet^2}{2\sigma^2}\right)$ where σ_ρ^2 is the parameter of the Rayleigh distribution and $2\sigma^2$ is the noise power in the range-bearing cell. We suppose that the target appears at time step $k_b = 10$ and disappears at time step $k_e = 75$. The total duration of the experiment is set to $k_{max} = 100$.

C. Single target TBD particle filter

We briefly present here the classic TBD particle filter for a single target case used for the simulations [7]. As the presence of the target at each iteration is unknown, a variable s_k is added to the particle state vector that takes value 1 if the target is present and 0 otherwise. This allows to compute the target probability of existence $P_k^e = p(s_k = 1 \mid \mathbf{z}_k)$. To keep the Markovian structure, $(s_k)_{k\in\mathbb{N}}$ follows a Markov chain with transition probabilities $P_b = p(s_k = 1 \mid s_{k-1} = 0)$ (birth probability) and $P_d = p(s_k = 0 \mid s_{k-1} = 1)$ (death probability). The particle target state of the p^{th} is only defined when $s_k^p = 1$. In that case, if $s_{k-1}^p = 1$ the particle target state $\mathbf{x}_k^p$ evolves according to the following linear equation:

$$\mathbf{x}_k^p = \mathbf{F}\mathbf{x}_{k-1}^p + \mathbf{v}_k^p, \tag{19}$$

where $\mathbf{v}_k^p$ is a white Gaussian noise with covariance matrix

$$\mathbf{Q} = \begin{bmatrix} \mathbf{Q}_s & 0 \\ 0 & \mathbf{Q}_s \end{bmatrix}, \text{ with } \mathbf{Q}_s = q_s \begin{bmatrix} T^3/3 & T^2/2 \\ T^2/2 & T \end{bmatrix},$$

and $\mathbf{F}$ is the transition matrix defined by:

$$\mathbf{F} = \begin{bmatrix} \mathbf{F}_s & 0 \\ 0 & \mathbf{F}_s \end{bmatrix} \text{ with } \mathbf{F}_s = \begin{bmatrix} 1 & T \\ 0 & 1 \end{bmatrix}.$$

Here T represents the sampling period of the measurement. If $s_{k-1}^p = 0$, the target state is drawn uniformly over its definition set:

- the position $[x_k^p, y_k^p]$ is uniformly distributed in the radar observation window;
- the velocity $[\dot{x}_k^p, \dot{y}_k^p]$ is uniformly distributed in the area $\mathcal{C} = \{(\dot{x}_k^p, \dot{y}_k^p) \mid v_{min} \leqslant \sqrt{(\dot{x}_k^p)^2 + (\dot{y}_k^p)^2} \leqslant v_{max}\}$.

As for the parameter σ_ρ^2, we use the method proposed in [11] to estimate it and therefore sample it with the particles. For the birth case, this parameter is uniformly distributed over the interval corresponding to a target SNR between SNR_{min} and SNR_{max} while for the survival case, the parameter is propagated with variance σ_n^2.

At each iteration, the particle filter propagates N_c particles (continuing particles) according to equation (19) (from previous iteration) and initializes N_b new particles (birth particles) in the radar observation window. Note that initializing the particle positions with the prior is not relevant, and we prefer using the instrumental density proposed in [13] that initializes particle positions in the cells that exceed a given threshold $\nu_{P_{f\bullet}} = -2\sigma^2 \log(P_{fa})$ [13] (where P_{fa} is a given probability of false alarm). Then it is possible to compute unnormalized weights for the p^{th} continuing and the q^{th} birth particles as:

$$\begin{aligned} \tilde{w}_{k,p}^c &= \frac{1}{N_c}\mathcal{L}(\mathbf{z}_k \mid \mathbf{x}_k^p), \\ \tilde{w}_{k,q}^b &= \frac{N_{P_{fa}}}{N} \times \frac{1}{N_b}\mathcal{L}(\mathbf{z}_k \mid \mathbf{x}_k^q), \end{aligned} \tag{20}$$

where $N_{P_{f\bullet}}$ is the number of cells exceeding the threshold $\nu_{P_{f\bullet}}$. The approximate posterior density can be seen as a mixture with two components, one for the birth particles and the other one for the continuing particles. The probability of each component is given by,

$$p_c = \frac{\tilde{M}_c}{\tilde{M}_c + \tilde{M}_b}, \qquad (21)$$
$$p_b = 1 - p_c,$$

where

$$\tilde{M}_c = (1 - P_d)\hat{P}^e_{k-1} \sum_{p=1}^{N_c} \tilde{w}^c_{k,p},$$
$$\tilde{M}_b = P_b(1 - \hat{P}^e_{k-1}) \sum_{q=1}^{N_b} \tilde{w}^b_{k,q}, \qquad (22)$$

with $\hat{P}^e_{k-1}$ the estimated probability of target existence at step $k-1$. Finally the estimated probability $\hat{P}^e_k$ of target existence can be computed from these quantities by

$$\hat{P}^e_k = \frac{\tilde{M}_c + \tilde{M}_b}{\tilde{M}_c + \tilde{M}_b + P_d\hat{P}^e_{k-1} + (1 - P_b)(1 - \hat{P}^e_{k-1})}. \qquad (23)$$

The unnormalized weights are then normalized such that the sum of the normalized weights equals p_c for the continuing particles and equals p_b for the birth particles. Finally, N_c particles are resampled from the $N_c + N_b$ particle cloud.

D. Simulations

The target SNR is fixed to 5dB. For the simulations the following parameters are used: $T = 1$ s, $v_{min} = 0.1\,\mathrm{km.s^{-1}}$, $v_{max} = 0.3\,\mathrm{km.s^{-1}}$, $\mathrm{SNR}_{min} = 2\,\mathrm{dB}$, $\mathrm{SNR}_{max} = 20\,\mathrm{dB}$, $q_s = 10^{-3}$,$P_{fa} = 0.1$ and $\sigma_n^2 = 0.1$. The transition probabilities for the jump Markov process are set to $P_b = P_d = 0.05$. We choose $N_c = 2000$ and $N_b = 1000$. For the simulation of the radar measurements, we use: $r_{min} = 100\,\mathrm{km}$, $r_{max} = 120\,\mathrm{km}$, $\Delta_r = 0.5\,\mathrm{km}$, $\theta_{min} = -10°$, $\theta_{max} = +10°$, $\Delta_\theta = 1.45°$, $N_r = 40$, $N_\theta = 14$, $\mathbf{\Gamma} = 2\sigma^2\mathbf{I}_N$ with $\sigma^2 = 0.5$, $B = 150\,\mathrm{kHz}$, $T_e = 6.67 \times 10^{-5}\,\mathrm{s}$, $N_a = 70$, $\lambda = 3\,\mathrm{cm}$, $c = 3 \times 10^8\,\mathrm{m.s^{-1}}$. Note that a small radar window is chosen here to avoid using an important number of particles.

We estimate the probability of presence, the probability of detection and the Root Mean Square Error (RMSE) in position and velocity via $N_{MC} = 5000$ Monte-Carlo runs. These quantities are computed for the two following filters: the first one computes particle weights from the square modulus of the complex measurement and is denoted by SMPF, while the second one computes the particle weights directly from the complex measurement and is denoted by CMPF. Then, the probability of presence is directly provided by each particle filter and averaged over the N_{MC} simulations. We propose the following detection strategy based on this probability of presence. Let us call d_k the decision at time step k that can take value 0 (no detection) or 1 (detection). We propose to take the decision by thresholding the probability $\hat{P}^e_k$ with an adaptive threshold $T(d_{k-1})$ depending on the previous decision d_{k-1} ($d_k = 1$ if $\hat{P}^e_k > T(d_{k-1})$). As the value of the estimator $\hat{P}^e_{k-1}$ can take low values, this avoids to declare no detection whereas the position estimated by the filter is very close to the actual target position. For the simulation, $T(d_{k-1} = 1)$ is set to 0.2 and $T(d_{k-1} = 0)$ is set to 0.9. Then, we estimate the false alarm probability $P_{fa,k}$ as follows. When the target is absent, it is the average over the N_{MC} simulations of the detection variable d_k and when the target is present, it is the average of the variable d_k where the estimated position of the target is outside a vicinity of two range-bearing cells from the actual target position. The target detection probability $P_{D,k}$ at step k is obtained in a similar way: when the target is present, it is the mean of the variable d_k where the estimated position of the target is located in a vicinity of two range-bearing cells from the real target position. Finally the RMSEs in position and velocity are calculated only when the detection variable d_k is equal to 1 and when the estimated position of the target is located in a vicinity of two range-bearing cells from the real target position. We present in figure 1 the performance of the two filters in terms of estimated probability of presence and in terms of probability of detection and false alarm. In figure 2 we present the performances in terms of RMSE in position and in velocity for the two filters. Clearly, the filter that computes the weights from the complex measurement provides much better performance than the filter using the square modulus of the complex signal.

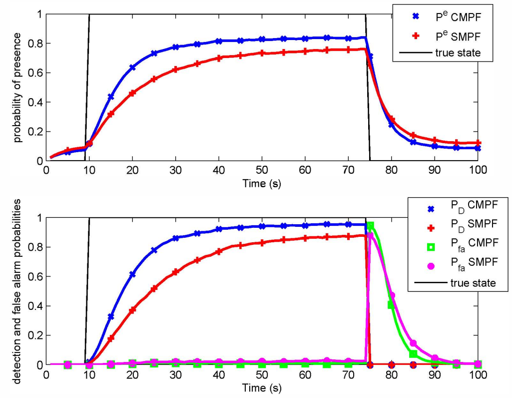

Fig. 1. Monte-Carlo simulations results for the single target case with the *Swerling* 1 model. Top: average probability of presence. Bottom: detection and false alarm probabilities. SNR $= 5\,\mathrm{dB}$.

VI. Multi-target simulations and results

We consider in this section the crossing of two targets that follow rectilinear trajectories. The angle between the two velocity target vectors is set to $\frac{\pi}{4}$. We denote by d_{min} the minimum distance between the two targets and assume that it is reached at time step k_c.

A. Multi-target particle filter

We used for these simulations the multi-target particle filter proposed by Kreucher *et al.* in [4]. This filter allows to estimate the number of targets. However as we are concerned here mainly by the likelihood computation when the targets are close to each other, we assume that the number of targets is known. So the particle filter is composed of N_p multi-target particle state vectors that contain two targets, *i.e.* each particle state vector is defined by $\mathbf{X}^p_k = [\mathbf{x}^p_{k,1}, \mathbf{x}^p_{k,2}]^T$ where $\mathbf{x}^p_{k,1}$ is the single state vector belonging to the first target and $\mathbf{x}^p_{k,2}$ is the single state vector belonging to the second target. Moreover, we assume that the tracks have already been initialized, so that at step $k = 0$ each target state $\mathbf{x}^p_{0,i}$ of particle p is initialized from the actual target state. This initialization is

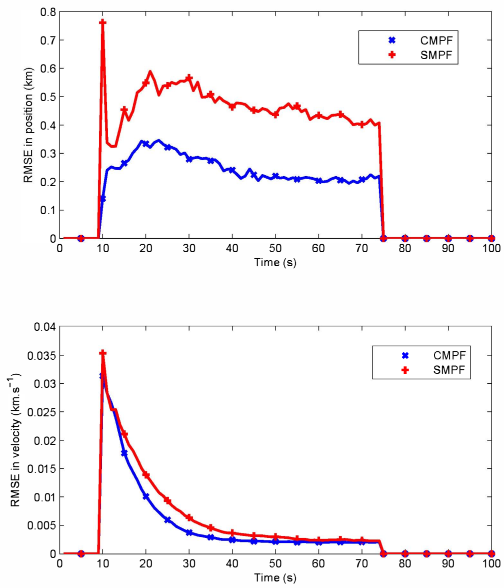

Fig. 2. Monte-Carlo simulations results for the single target case with the *Swerling* 1 model. Top: RMSE in position. Bottom: RMSE in velocity. SNR = 5 dB.

done as follows: for the position we add a small Gaussian noise with variance σ_r^2 on the actual target range $r_{0,i} = \sqrt{x_{0,i}^2 + y_{0,i}^2}$ and a small Gaussian noise with variance σ_θ^2 on the true target bearing $\theta_{0,i} = \arctan\left(\frac{y_{0,i}}{x_{0,i}}\right)$. For the velocity, we initialize it around the true velocity in Cartesian coordinates and we add a small Gaussian noise with covariance matrix $\sigma_v^2 \mathbf{I}_2$. For the particle propagation, we use as instrumental density the Independent Partition (IP) method defined by Kreucher *et al.* [4]. This method consists in computing likelihood ratios separately for each target when they are well separated and sample the state of the particles according to the distributions defined by the likelihood ratios of each target. In the other case, *i.e.* when target are too close to each other, we just propagate particles according to the prior distribution (19). Finally the particle filter used can be summarized as follows: first, at step $k = 0$, initialize particles from the actual target positions. Then, propagate particles according to IP if particles belonging to each target are sufficiently disjoint, or according to the prior if not, and finally compute weights and resample.

B. Simulations

For the simulations, the SNR is set to 10 dB for each target. The trajectories of both targets are randomly simulated such that their velocity vector form an angle of $\frac{\pi}{4}$ and cross at step $k_c = 35$ with $d_{min} = 0.5$ km. For the filter we use the following parameters: $T = 1$ s, $q_s = 10^{-3}$, $\sigma_r^2 = 0.0625$, $\sigma_\theta^2 = 3.9952 \times 10^{-5}$, $\sigma_v^2 = 0.01$ and $\sigma_n^2 = 0.1$. For the simulation of the radar measurements, we use: $r_{min} = 100$ km, $r_{max} = 150$ km, $\Delta_r = 0.5$ km, $\theta_{min} = -20°$, $\theta_{max} = +20°$, $\Delta_\theta = 0.72°$, $N_r = 40$, $N_\theta = 56$, $\mathbf{\Gamma} = 2\sigma^2 \mathbf{I}_N$ with $\sigma^2 = 0.5$, $B = 150$ kHz, $T_e = 6.67 \times 10^{-5}$ s, $N_a = 140$, $\lambda = 3$ cm, $c = 3 \times 10^8$ m.s^{-1}.

The mean RMSE of the two targets in position and velocity and the probability of track loss are estimated from $N_{MC} = 2000$ Monte-Carlo runs. These quantities are estimated both for the *Swerling* 0 model and the *Swerling* 1 model. For the *Swerling* 0 model we use three different particle filters:

- The first one that uses the complex measurement to compute the weights. When the targets are too close to be supposed independent, the likelihood ratio is approximated with a numerical integration over $[0, 2\pi)^2$ and we use 20 samples per interval; we denote this filter by IntPF SW0.
- The second one that uses also complex measurement but when the targets are too close, the likelihood ratio is approximated with the strategy based on importance sampling (14). We set $N_{IS} = 1$ and $\delta_\varphi = \frac{\pi}{5}$; we denote this filter by ISPF SW0.
- The third filter that computes the weights according to the square modulus measurement; we denote this filter SMPF SW0.

For the *Swerling* 1 model, we use two different particle filters:

- The first one that uses the complex measurement to compute the weights with the equation (18); we denote this filter CMPF SW1.
- The second one that uses the square modulus measurement to compute the weights; we denote this filter SMPF SW1.

Note that in the case of close targets, assuming independent targets would lead to poor performance. At each iteration, we obtain an estimator of the target state for each target:

$$\hat{\mathbf{x}}_{k,i} = \frac{1}{N_p} \sum_{p=1}^{N_p} \mathbf{x}_{k,i}^p, \;\; i \in \{1, 2\},$$

and we associate each estimator to a target such that the sum of the Euclidean distances between the estimates and the actual state is minimum. Finally, we take for the RMSE (in position and velocity) the mean of the RMSE of the two targets. To evaluate the probability of track loss, we use the following methodology. For each Monte-Carlo run, at each time step k and for each target, we compute the loss variable $l_{k,i}$ that takes value 1 (target loss) if,

$$\begin{pmatrix} \hat{r}_{k,i} - r_{k,i} \\ \hat{\theta}_{k,i} - \theta_{k,i} \end{pmatrix} \mathbf{P} \begin{pmatrix} \hat{r}_{k,i} - r_{k,i} \\ \hat{\theta}_{k,i} - \theta_{k,i} \end{pmatrix} > \alpha,$$

and 0 otherwise. We define $\hat{r}_{k,i} = \sqrt{\hat{x}_{k,i}^2 + \hat{y}_{k,i}^2}$ as the range estimator and $\hat{\theta}_{k,i} = \arctan\left(\frac{\hat{y}_{k,i}}{\hat{x}_{k,i}}\right)$ as the bearing estimator, $\mathbf{P} = \begin{pmatrix} \frac{1}{\Delta_r} & 0 \\ 0 & \frac{1}{\Delta_\theta} \end{pmatrix}$ and $\alpha = 5.99$ is the value of the quantile function of the chi-square distribution with two degrees of freedom evaluated at 0.95. In other words, at each iteration, we check if the position estimator for each target is located within the 0.95% confidence ellipse around the true target position. Finally, a track is declared to be lost if at least one of the variables $l_{k,i}$ equals 1 during at least five consecutive iterations. We define f_m the loss variable for the m^{th} Monte-Carlo run that takes value 1 if the filter failed to track the two targets during all the experiment and 0, otherwise. Then, the

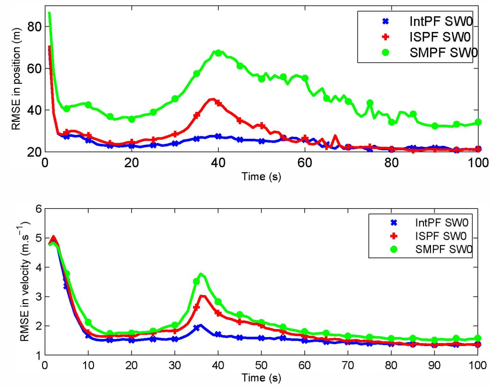

Fig. 3. Monte-Carlo simulations results in a multi-target setting with the *Swerling* 0 model. Top: RMSE in position. Bottom: RMSE in velocity.

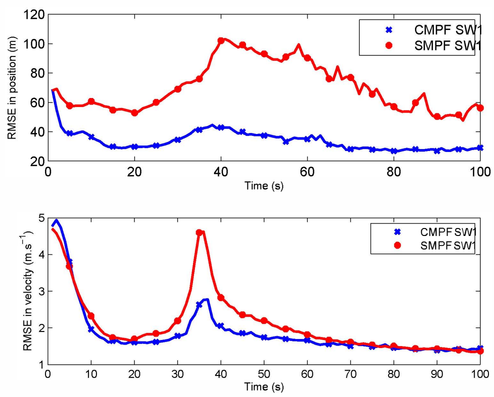

Fig. 4. Monte-Carlo simulations results in a multi-target setting with the *Swerling* 1 model. Top: RMSE in position. Bottom: RMSE in velocity.

probability of track loss is given by $\hat{P}_{loss} = \frac{1}{N_{MC}} \sum_{m=1}^{N_{MC}} f_m$. We present in figure 3 the performance in terms of RMSE in position and velocity for the three filters in the *Swerling* 0 case. For the *Swerling* 1 model, the performance in terms of RMSE in position and velocity is presented in figure 4. We can notice that the RMSE tends to increase around time sample 40 seconds. This corresponds to the moment where the targets are the closest. Finally, we provide in table I the probability of track loss for all the filters considered in this section. As for the single target case, filters that compute the weights according to the complex measurement provide much better performance than filters that work with the square modulus of the complex signal. Note also that the performance is slightly better for the *Swerling* 0 model than for the *Swerling* 1 model. Indeed, as the modulus fluctuates, the instantaneous SNR may take low values, thus making the tracking more difficult.

VII. Conclusion

In this paper, we have proposed different methods for computing the likelihood of the complex raw radar data that take into account the spatial coherence of the target complex amplitudes. For the *Swerling* 0 model, we have presented two approximations for computing the likelihood of the complex measurement in a multi-target setting. For the *Swerling* 1 case,

	Probability of track loss
IntPF SW0	1×10^{-3}
ISPF SW0	1×10^{-3}
SMPF SW0	4.6×10^{-3}
CMPF SW1	6×10^{-3}
SMPF SW1	2.41×10^{-2}

TABLE I. Estimated probability of track loss for the different multi-target particle filters considered.

we have shown that a closed form can be obtained to compute the multi-target likelihood of the complex measurement. Finally, we have demonstrated with Monte-Carlo simulations the benefits of taking into account the spatial coherence of the complex amplitudes both in detection and in estimation compared to the classic method that works on the square modulus of the complex signal.

References

[1] Y. Boers, F. Ehlers, W. Koch, T. Luginbuhl, L.D. Stone, and R.L. Streit. *Track Before Detect Algorithms*. Eurasip Journal on Applied Signal Processing, 2008.

[2] T.E. Fortmann, Y. Bar-Shalom, and M. Scheffe. Sonar tracking of multiple targets using joint probabilistic data association. *IEEE Journal of Oceanic Engineering*, 8(3):173–184, 1983.

[3] D.J. Salmond and H. Birch. A particle filter for track-before-detect. In *Proc. American Control Conf.*, pages 3755–3760, 2001.

[4] C. Kreucher, K. Kastella, and A.O. Hero. Multitarget Tracking using the Joint Multitarget Probability Density. *IEEE Trans. on Aerospace and Electronic Systems*, 41(4):1396–1414, 2005.

[5] M.S. Arulampalam, S. Maskell, N. Gordon, and T. Clapp. A tutorial on particle filters for online nonlinear/non-Gaussian Bayesian tracking. *IEEE Transactions on Signal Processing*, 50(2):174 –188, Feb. 2002.

[6] M.I. Skolnik. *Introduction to radar systems*. McGraw-Hill, New York, 1962.

[7] M.G. Rutten, B. Ristic, and N.J. Gordon. A comparison of particle filters for recursive track-before-detect. In *7th Int. Conf. on Information Fusion*, pages 169–175, 2005.

[8] Y. Boers and J.N. Driessen. Multitarget particle filter track-before-detect application. In *IEE Proc. Radar Sonar Navig.*, volume 151, pages 351–357, 2004.

[9] S.J. Davey, M.G. Rutten, and B. Cheung. Using phase to improve track-before-detect. *IEEE Transactions on Aerospace and Electronic Systems*, 48(1):832 –849, Jan. 2012.

[10] M.G. Rutten, N.J. Gordon, and S. Maskell. Recursive track-before-detect with target amplitude fluctuations. *Radar, Sonar and Navigation, IEE Proceedings* -, 152(5):345 – 352, Oct. 2005.

[11] C. Andrieu, A. Doucet, S.S. Singh, and V.B. Tadic. Particle methods for change detection, system identification, and control. *Proceedings of the IEEE*, 92(3):423–438, 2004.

[12] H.L. Van Trees. *Optimum Array Processing, Part IV of Detection, Estimation, and Modulation Theory*. John Wiley and Sons, 2002.

[13] A. Lepoutre, O. Rabaste, and F. Le Gland. Optimized instrumental density for particle filter in track-before-detect. In *9th IET Data Fusion & Target Tracking Conference*, 2012.